

TRANSISTOR h PARAMETER MEASUREMENT
TECHNIQUES

By

DANIEL M. RUKAVINA

Bachelor of Science

Michigan College of Mining and Technology

Houghton, Michigan


1959

Submitted to the faculty of the Graduate School of
the Oklahoma State University
in partial fulfillment of the requirements
for the degree of
MASTER OF SCIENCE
August, 1962

NOV 13 1962


TRANSISTOR h PARAMETER MEASUREMENT
TECHNIQUES

Thesis Approved:



Thesis Adviser





Dean of the Graduate School

505227

PREFACE

An important area in the development of solid state devices and their applications to man's need is device characterization. It is necessary that persons engaged in solid state circuit design and device applications have a concise description of the electrical characteristics of the devices with which they are working. Device characterization is an important factor in circuit analysis and synthesis, and while design theory is not particularly useful for circuit applications, the value of a correlation between design theory and circuit theory may have a bearing on the manner in which the electrical performance of the device is characterized. At this point it is necessary to limit the scope of this study to a particular solid state device, the junction transistor and to consider circuit analysis as the prime factor in determining how a transistor will be characterized.

Much has been done in this area over the past five years, and it would be difficult if not impossible to mention any more than a small portion of the accomplishments. In general the aim of this study has been the simplification of parameter measurement techniques which are presently used in small signal, low frequency transistor equivalent circuit representation. The fourpole hybrid equivalent circuit has been chosen for this investigation. The hybrid parameters which by definition must be measured under prescribed impedance termination conditions were measured under less stringent termination conditions

with the hope that the resulting measurement errors could be corrected. The complex valued current gain parameter was measured in the common emitter configuration, and information gained from this measurement was used to approximate the transistor's current gain cutoff frequency.

The writer wishes to express his sincere appreciation to Dr. Harold T. Fristoe, thesis adviser, for his encouragement and assistance in guiding this study.

TABLE OF CONTENTS

Chapter	Page
I. INTRODUCTION	1
The Transistor as an Active Fourpole.	1
Derivation of Error Factors	8
II. COMMON EMITTER h PARAMETER MEASUREMENTS.	18
III. COMMON EMITTER h PARAMETER MEASUREMENT CIRCUITS.	26
h_{11} and h_{21} Measurement Circuit	26
h_{12} and h_{22} Measurement Circuit	28
IV. FREQUENCY DEPENDENCE OF h_{21}	31
Introduction.	31
A Bridge for Measuring h_{21}	33
Circuit Operation	37
V. CONSLUSION	40
BIBLIOGRAPHY,	43

LIST OF TABLES

Table	Page
I-1. h , y , and z Parameter Relations.	9
I-2. Error Factor Formulas for h Parameters	13
II-1. Results of h_{11} and h_{21} Measurements Under Various Termination Conditions.	23
II-2. Results of h_{12} and h_{22} Measurements Under Various Termination Conditions.	24

LIST OF FIGURES

Figure	Page
I-1. Fourpole	1
I-2. h_{11} and h_{21} Measurement Circuit.	10
I-3. h_{12} and h_{22} Measurement Circuit.	12
I-4. h_{22} Measurement Circuit.	14
I-5. h_{22} Measurement Circuit.	15
I-6. h_{22} Measurement Circuit.	16
II-1. h_{11} and h_{21} Measurement Circuit.	18
II-2. h_{12} and h_{22} Measurement Circuit.	20
III-1. h_{11} and h_{21} Measurement Circuit.	27
III-2. Collector Biasing Scheme	29
III-3. h_{12} and h_{22} Measurement Circuit.	29
IV-1. $R_e h_{21} + j I_m h_{21}$ Measurement Circuit.	33
IV-2. $R_e h_{21} + j I_m h_{21}$ Measurement Circuit.	35
IV-3. $R_e h_{21} + j I_m h_{21}$ Measurement Circuit.	35
IV-4. $R_e h_{21} + j I_m h_{21}$ Measurement Circuit.	36

CHAPTER I

INTRODUCTION

The Transistor as an Active Fourpole

General fourpole or two-port network theory can be used as a basis for equivalent circuit representation of transistors. The obvious advantage in this, of course, is to make use of the results of fourpole theory in transistor circuitry.

The prime concern in fourpole network theory is to find a relationship between terminal voltages and currents for the device or network which is to be represented. Since this can be done in several ways, we are generally concerned with selecting the most desirable fourpole relationship from the standpoint of ease with which parameter measurements can be made. Three of the six permutations in which the general linear fourpole equation can be written have found practical use in transistor applications.

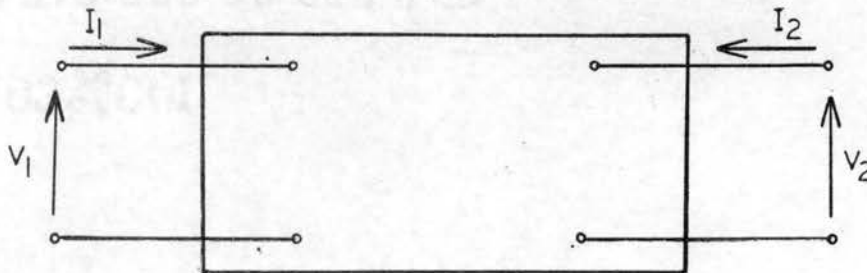


Figure I-1. Fourpole

The fourpole shown in Figure I-1 is drawn with the usual sign convention concerning currents and voltages. In general the voltages and currents V_1 , I_1 , V_2 , and I_2 are related by two independent implicit equations, the explicit form of which is governed by our selection of the independent variables.

$$V_1 = f_1 (I_1, V_2) \quad (\text{I-1})$$

$$I_2 = f_2 (I_1, V_2) \quad (\text{I-2})$$

$$V_1 = f_3 (I_1, I_2) \quad (\text{I-3})$$

$$V_2 = f_4 (I_1, I_2) \quad (\text{I-4})$$

$$I_1 = f_5 (V_1, V_2) \quad (\text{I-5})$$

$$I_2 = f_6 (V_1, V_2) \quad (\text{I-6})$$

The fourpole equation which is the result of the selection of independent variables I_1 and V_2 is represented by the h or hybrid equivalent circuit. The z parameter equivalent circuit and y parameter equivalent circuit depend upon the choice of I_1 and I_2 or V_1 and V_2 , respectively, as independent variables. The parameters are then represented by taking the total differential of the functional equations with certain physical restraints imposed. The parameters are generally denoted by the letter h, z, or y followed by a double subscript, the first number of which indicates whether the parameter is in the input or output portion of the equivalent circuit (1 refers to input, 2 refers

to output). The second number of the parameter subscript refers to the independent variable to which the parameter is related in the equivalent circuit.

The h or hybrid equivalent circuit is considered to have several advantages over the z and y equivalent circuits. Since the transistor is inherently a low input impedance and high output impedance device, the measurement of the h parameters can be made with very little difficulty. These measurements require open circuit input and short circuit output conditions. The open circuit input condition is not difficult to produce; since, as stated previously, the transistor is inherently a low input impedance device. In contrast the open circuit output condition which must be met in the measurement of the z parameters is difficult to obtain at a reasonable measuring frequency. The magnitude of the output impedance, z_{22} , may be in the meg-ohm range, hence open circuit conditions would require a hundred meg-ohm impedance in the output loop.

In addition to being more readily measured, the h parameters provide an insight into important factors governing transistor circuit performance. h_{11} and h_{22} provide information for impedance matching; h_{21} is the available current gain of the device; and h_{12} is a measure of the isolation and internal feedback performance of the device.

At this point it would be useful to consider in more detail the implications and limitations of fourpole theory as applied to transistor equivalent circuits. Dr. W. W. Gartner's (1) discussion of fourpole theory as applied to transistor equivalent circuits will be used as a guide in our development of the hybrid equivalent circuit. The primary reason for choosing the h parameter equivalent circuit was the

conclusion of H. G. Follingstad (2) in "An Analytical Study of z , y , and h Parameter Accuracies in Transistor Sweep Measurement:"

... at low frequencies the most generally useful and accurate sweep measurements are obtained with hybrid (h) parameters.

The possibility that the functional relationships given in Equations (I-1) and (I-2) might each contain an infinite number of terms does not alter the fact that two independent equations in four unknowns may be solved for a pair of unknowns each expressed explicitly in terms of the other two. However, the resulting expressions may still contain an infinite number of terms. Regardless of whether or not f_1 and f_2 are closed form functions with finite numbers of terms, the relationships between I_1 , V_2 and V_1 or I_2 can be determined graphically. Sets of curves which picture these relationships are called static characteristics since they are valid only for d.c. and low frequency transistor operation. The problem of expressing the relationship between the current and voltage variables is further complicated by the requirement that the currents and voltages be functions of time. With this in mind we write the variables V_1 , I_1 , V_2 , and I_2 as $V_1(t)$, $I_1(t)$, $V_2(t)$, and $I_2(t)$. It is convenient to express the voltages and currents which are now time functions as the sum of a d.c. or steady state term and a second term which is time dependent. Hence we write $V_1(t)$, $I_1(t)$, $V_2(t)$, and $I_2(t)$ as $V_{01} + v_1(t)$, $I_{01} + i_1(t)$, $V_{02} + v_2(t)$, and $I_{02} + i_2(t)$. This is done because we wish to eliminate the d.c. components and consider only the time dependent components, $v_1(t)$, $i_1(t)$, $v_2(t)$, and $i_2(t)$. Since we are primarily interested in the hybrid equivalent circuit, we will use I_1 and V_2 as the independent variables

in this discussion. Equations (I-1) and (I-2) can be written in Taylor series expansions about arbitrary steady state values of V_1 , I_1 , V_2 , and I_2 . Let us denote these steady state voltages and currents by V_{01} , I_{01} , V_{02} , and I_{02} . First we rewrite Equations (I-1) and (I-2) incorporating the notation mentioned previously, and then we use a Taylor series expansion about V_{01} , I_{01} , V_{02} , and I_{02} to eliminate the d.c. terms from our equations. The resulting expressions form the basis for the definition of the h parameters.

$$V_1(t) = V_{01} + v_1(t) = f_1 [I_{01} + i_1(t), V_{02} + v_2(t)] \quad (\text{I-7})$$

$$I_2(t) = I_{02} + i_2(t) = f_2 [I_{01} + i_1(t), V_{01} + v_1(t)] \quad (\text{I-8})$$

Equation (I-7) can be written

$$\begin{aligned} V_1(t) = V_{01} + v_1(t) = & f_1(I_{01}, V_{02}) + \left. \frac{\partial f_1}{\partial I_1} \right]_{I_{01}, V_{02}} [i_1(t)] \\ & + \left. \frac{\partial f_1}{\partial V_2} \right]_{I_{01}, V_{02}} [v_2(t)] + \left. \frac{1}{2} \frac{\partial^2 f_1}{\partial I_1^2} \right]_{I_{01}, V_{02}} [i_1(t)]^2 \\ & + \left. \frac{1}{2} \frac{\partial^2 f_1}{\partial V_2^2} \right]_{I_{01}, V_{02}} [v_2(t)]^2 + \left. \frac{\partial^2 f_1}{\partial I_1 \partial V_2} \right]_{I_{01}, V_{02}} [i_1(t)] [v_2(t)] + \dots \end{aligned} \quad (\text{I-9})$$

Similarly

$$\begin{aligned} I_2(t) = I_{02} + i_2(t) = & f_2(I_{01}, V_{02}) + \left. \frac{\partial f_2}{\partial I_1} \right]_{I_{01}, V_{02}} [i_1(t)] \\ & + \left. \frac{\partial f_2}{\partial V_2} \right]_{I_{01}, V_{02}} [v_2(t)] + \left. \frac{1}{2} \frac{\partial^2 f_2}{\partial I_1^2} \right]_{I_{01}, V_{02}} [i_1(t)]^2 \end{aligned}$$

$$+ \frac{1}{2} \frac{\partial^2 f_2}{\partial v_2^2} \left[v_2(t) \right]^2 + \frac{\partial^2 f_2}{\partial I_1 \partial v_2} \left[i_1(t) \right] \left[v_2(t) \right] + \dots \quad (I-10)$$

If $i_1(t)$ and $v_2(t)$ are limited to small amplitudes, the terms containing $i_1(t)$ and $v_2(t)$ of order higher than one can be neglected without introducing appreciable error in Equations (I-9) and (I-10).

Since $v_{01} = f_1(I_{01}, V_{02})$, Equation (I-9) can be written

$$v_1(t) = \frac{\partial f_1}{\partial I_1} \left[i_1(t) \right] + \frac{\partial f_1}{\partial v_2} \left[v_2(t) \right] \quad (I-11)$$

Similarly Equation (I-10) can be written

$$i_2(t) = \frac{\partial f_2}{\partial I_1} \left[i_2(t) \right] + \frac{\partial f_2}{\partial v_2} \left[v_2(t) \right] \quad (I-12)$$

Dr. W. W. Gartner (3) in Transistors: Principles, Design and Applications states:

...for each individual frequency the proportionality constants, $\frac{\partial f_1}{\partial I_1}$, $\frac{\partial f_2}{\partial I_1}$, ... etc., are independent of time and only a function of frequency.

This implies that Equations (I-11) and (I-12) may be written

$$v_1(t) = h_{11}(\omega, I_{01}, V_{02}) [i_1(t)] + h_{12}(\omega, I_{01}, V_{02}) [v_2(t)] \quad (I-13)$$

$$i_2(t) = h_{21}(\omega, I_{01}, V_{02}) [i_1(t)] + h_{22}(\omega, I_{01}, V_{02}) [v_2(t)] \quad (I-14)$$

Where ω is angular frequency, and

$$\begin{aligned}
 h_{11}(\omega, I_{01}, V_{02}) &= \left. \frac{\partial f_1}{\partial I_1} \right|_{I_{01}, V_{02}} \\
 h_{12}(\omega, I_{01}, V_{02}) &= \left. \frac{\partial f_1}{\partial V_2} \right|_{I_{01}, V_{02}} \\
 h_{21}(\omega, I_{01}, V_{02}) &= \left. \frac{\partial f_2}{\partial I_1} \right|_{I_{01}, V_{02}} \\
 h_{22}(\omega, I_{01}, V_{02}) &= \left. \frac{\partial f_2}{\partial V_2} \right|_{I_{01}, V_{02}}
 \end{aligned} \tag{I-15}$$

The dependence of the h parameters on frequency, bias point, and the fact that they are valid only for small signals is implied when they are written in short hand fashion.

$$v_1 = h_{11} i_1 + h_{12} v_2 \tag{I-16}$$

$$i_2 = h_{21} i_1 + h_{22} v_2 \tag{I-17}$$

Hence the h parameters at a particular quiescent point, (I_{01}, V_{02}) , are often defined in the following manner:

$$\begin{aligned}
 h_{11} &= \left. \frac{v_1}{i_1} \right|_{v_2 = 0} \\
 h_{12} &= \left. \frac{v_1}{v_2} \right|_{i_1 = 0} \\
 h_{21} &= \left. \frac{i_2}{i_1} \right|_{v_2 = 0} \\
 h_{22} &= \left. \frac{i_2}{v_2} \right|_{i_1 = 0}
 \end{aligned} \tag{I-18}$$

Derivation of Error Factors

In order to make use of the equations given in (I-16) and (I-17), we must be able to determine either graphically or experimentally the parameters which appear in these equations. If this is to be done experimentally, we see from Equation (I-18) that current and voltage measurements must be made with a zero impedance termination on the output ($v_2 = 0$) when h_{11} and h_{21} are being determined, and an infinite impedance termination on the input ($i_1 = 0$) when h_{12} and h_{22} are being determined. Since measurements are generally made with non-zero, finite terminations, errors in measurement are unavoidable. The procedure suggested by H. G. Follingstad (4) will be used to compensate for measurement errors.

The derivation of the correction factors for the h parameter representation is simplified somewhat by using z, y, and h fourpole equations and the relationships between the z, y, and h parameters. These relationships are tabulated below for reference purposes.

The defining equations for the z parameters are:

$$v_1 = z_{11} i_1 + z_{12} i_2 \quad (\text{I-19})$$

$$v_2 = z_{21} i_1 + z_{22} i_2 \quad (\text{I-20})$$

The defining equations for the y parameters are:

$$i_1 = y_{11} v_1 + y_{12} v_2 \quad (\text{I-21})$$

$$i_2 = y_{21} v_1 + y_{22} v_2 \quad (\text{I-22})$$

Generally two sources of measurement error exist, a termination

TABLE I-1

h, y, AND z PARAMETER RELATIONS (4)

z_{11}	$1/y_{11}(1 - \tau)$	$h_{11}/(1 - \tau)$
z_{12}	$-y_{12}/y_{11} y_{22}(1 - \tau)$	h_{12}/h_{22}
z_{21}	$-y_{21}/y_{11} y_{22}(1 - \tau)$	$-h_{21}/h_{22}$
z_{22}	$1/y_{22}(1 - \tau)$	$1/h_{22}$
$1/z_{11}(1 - \tau)$	y_{11}	$1/h_{11}$
$-z_{12}/z_{11} z_{22}(1 - \tau)$	y_{12}	$-h_{12}/h_{11}$
$-z_{21}/z_{11} z_{22}(1 - \tau)$	y_{21}	h_{21}/h_{11}
$1/z_{22}(1 - \tau)$	y_{22}	$h_{22}/(1 - \tau)$
$z_{11}(1 - \tau)$	$1/y_{11}$	h_{11}
z_{12}/z_{22}	$-y_{12}/y_{11}$	h_{12}
$-z_{21}/z_{22}$	y_{21}/y_{11}	h_{21}
$1/z_{22}$	$y_{22}/(1 - \tau)$	h_{22}
$\tau = z_{21} z_{12}/z_{11} z_{22}$	$\tau = y_{21} y_{12}/y_{11} y_{22}$	$\tau = \frac{1}{1 - h_{11} h_{22}/h_{21} h_{12}}$

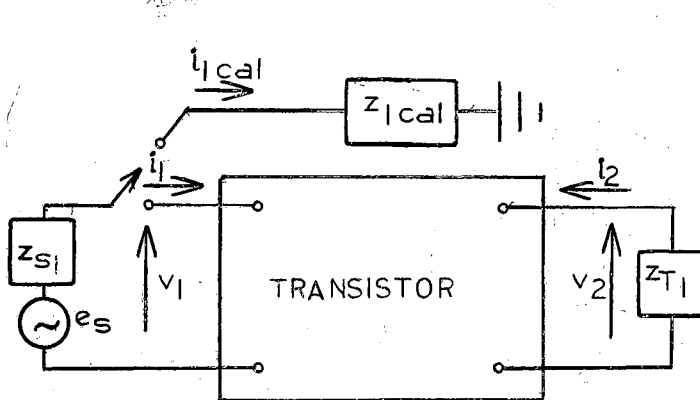
error and a calibration error.

Dividing Equation (I-16) by i_1 we obtain

$$\frac{v_1}{i_1} = h_{11} + h_{12} \frac{v_2}{i_1} \quad (\text{I-23})$$

The additive term, $h_{12} \frac{v_2}{i_1}$, induces an error in the h_{11} measurement which will be compensated for by a "termination error factor," hereafter referred to as T.E.F. A further source of error is introduced when the test signal deviates from a calibrated signal. In measuring h_{11} the ratio of i_1 to $i_{1 \text{ cal}}$ (see Figure I-2 and Equation (I-26)) is a "source error factor," hereafter referred to as S.E.F., multiplying $\frac{v_1}{i_1}$.

As Equations (I-18) imply, there are two h parameter measuring circuits. The one for which $v_2 \rightarrow 0$ yields h_{11} and h_{21} (see Figure I-2), and the other for which $i_1 \rightarrow 0$ yields h_{12} and h_{22} (see Figure I-3). Since there is a S.E.F. and T.E.F. associated with each parameter, the h parameter subscript will be used to distinguish between error factors; i.e., T.E.F.₁₁ is the termination error factor for the parameter h_{11} . The derivations of T.E.F.₁₁ and S.E.F.₁₁ follow:



$$\frac{v_1}{i_{1 \text{ cal}}} = \underbrace{\left(\frac{i_1}{i_{1 \text{ cal}}} \right)}_{\text{S.E.F.}_{11}} \left(\frac{v_1}{i_1} \right)$$

$$\frac{v_1}{i_1} = \underbrace{\left(1 + \frac{h_{12} v_2}{h_{11} i_1} \right)}_{\text{T.E.F.}_{11}} h_{11}$$

$$h_{11} = \frac{v_1 / i_{1 \text{ cal}}}{(\text{S.E.F.}_{11}) \cdot (\text{T.E.F.}_{11})}$$

Figure I-2. h_{11} and h_{21} Measurement Circuit

Dividing Equation (I-20) by i_1 yields

$$\frac{v_2}{i_1} = z_{21} + z_{22} \frac{i_2}{i_1} \quad (I-24)$$

From Figure I-2, $i_2 = -\frac{v_2}{z_{T1}}$, hence Equation (I-24) can be written

$$\frac{v_2}{i_1} = z_{21} - \left(\frac{z_{22}}{z_{T1}} \right) \frac{v_2}{i_1} \quad (I-24a)$$

Solving Equation (I-24a) for $\frac{v_2}{i_2}$ and substituting this value in Equation (I-23), we obtain

$$\frac{v_1}{i_1} = h_{11} + \frac{h_{12} z_{21}}{\left(1 + \frac{z_{22}}{z_{T1}} \right)} \quad (I-25)$$

Manipulation of Equation (I-25) using h-z parameter relationships given in Table I-1 yields

$$\frac{v_1}{i_1} = h_{11} \left[1 - \left(\frac{h_{21} h_{12}}{h_{11} h_{22}} \right) \left(\frac{1}{1 + \frac{1}{h_{22} z_{T1}}} \right) \right] \quad (I-25a)$$

Hence T.E.F.₁₁ is

$$1 - \left(\frac{h_{21} h_{12}}{h_{11} h_{22}} \right) \left(\frac{1}{1 + \frac{1}{h_{22} z_{T1}}} \right)$$

A similar analysis applied to Equation (I-17) divided by i_1 yields the T.E.F. for the measurement of h_{21} . This result is given in Table I-2. The S.E.F. for the measurement of h_{11} follows:

From Figure I-2

$$i_{1 \text{ cal}} = \frac{e_s}{z_{s1} + z_{1 \text{ cal}}} \quad (\text{I-26})$$

And

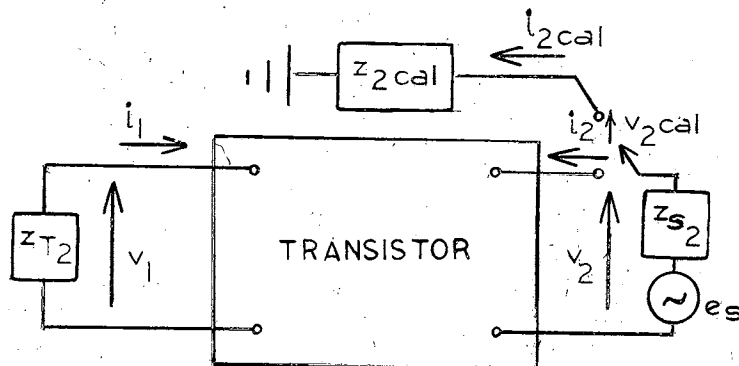
$$i_1 = \frac{e_s}{\left(z_{s1} + \frac{v_1}{i_1} \right)} \quad (\text{I-27})$$

Therefore

$$\frac{i_1}{i_{1 \text{ cal}}} = \text{S.E.F.}_{11} = \frac{z_{s1} + z_{1 \text{ cal}}}{z_{s1} + h_{11}} \quad (\text{I-28})$$

If the calibrating impedance, $z_{1 \text{ cal}}$, is not changed, $\text{S.E.F.}_{21} = \text{S.E.F.}_{11}$.

Derivations for the h_{12} and h_{22} error factors follow a similar pattern as those for h_{11} and h_{22} . The major difference is illustrated in Figure I-3. The driving signal is now applied to the output terminals and i_1 is forced to approach zero. In this case the y parameter Equation (I-21) is used in the derivation rather than the parameter Equation (I-20).



$$\frac{i_2}{v_{2 \text{ cal}}} = \frac{\left(\frac{v_2}{v_{2 \text{ cal}}} \right) \left(\frac{i_2}{v_2} \right)}{\text{S.E.F.}_{22}}$$

$$\frac{i_2}{v_2} = \frac{\left(1 + \frac{h_{21} i_1}{h_{22} v_2} \right) h_{22}}{\text{T.E.F.}_{11}}$$

$$h_{22} = \frac{i_2 / v_{2 \text{ cal}}}{(\text{S.E.F.}_{22}) (\text{T.E.F.}_{22})}$$

Figure I-3. h_{12} and h_{22} Measurement Circuit

TABLE I-2

ERROR FACTOR FORMULAS FOR h PARAMETERS

Measured Value	Source Error Factor (S.E.F.)	Termination Error Factor (T.E.F.)	Parameter
$\frac{v_1}{i_{1 \text{ cal}}}$	$\frac{z_{s1} + z_{1 \text{ cal}}}{z_{s1} + h_{11}}$	$1 - \left(\frac{h_{12} h_{21}}{h_{11} h_{22}} \right) \left(\frac{1}{1 + \frac{1}{h_{22} z_{T1}}} \right)$	h_{11}
$\frac{v_1}{v_{2 \text{ cal}}}$	$\frac{\left(1 - \frac{z_{s2}}{z_{s2} + i/h_{22}} \right)}{\frac{z_{2 \text{ cal}}}{z_{s2} + z_{2 \text{ cal}}}}$	$1 - \frac{1}{\left(1 + \frac{z_{T2}}{h_{11}} \right)}$	h_{12}
$\frac{i_2}{i_{1 \text{ cal}}}$	$\frac{z_{s1} + z_{1 \text{ cal}}}{z_{s1} + h_{11}}$	$1 - \frac{1}{\left(1 + \frac{1}{h_{22} z_{T1}} \right)}$	h_{21}
$\frac{i_2}{v_{2 \text{ cal}}}$	$\frac{\left(1 - \frac{z_{s2}}{z_{s2} + 1/h_{22}} \right)}{\frac{z_{2 \text{ cal}}}{z_{s2} + z_{2 \text{ cal}}}}$	$1 - \left(\frac{h_{21} h_{12}}{h_{22} h_{11}} \right) \left(\frac{1}{1 + \frac{z_{T2}}{h_{11}}} \right)$	h_{22}

Since the error factors given in Table I-2 are functions of the measured h parameters, the new set of parameters obtained by correction of the measured parameters is simply a better approximation of the actual values. Accuracy of the calculated set of parameters is obviously to some degree a function of how accurately the parameters were measured initially. Experimental results comparing measured and calibrated parameters for several termination conditions are given in the following chapter.

In the derivations of the error factors it was assumed that all necessary a.c. voltage and current measurements could be made without introducing additional errors. This is essentially true for all current and voltage measurements with the exception of i_2 , (see Figure I-3). i_2 is generally measured with a current sampling resistor which can be inserted in one of two positions in the circuit of Figure I-3. To predict the effect of this resistor on the measurement of h_{22} , consider first the two possible methods of i_2 measurement shown in Figure I-4 and Figure I-5.

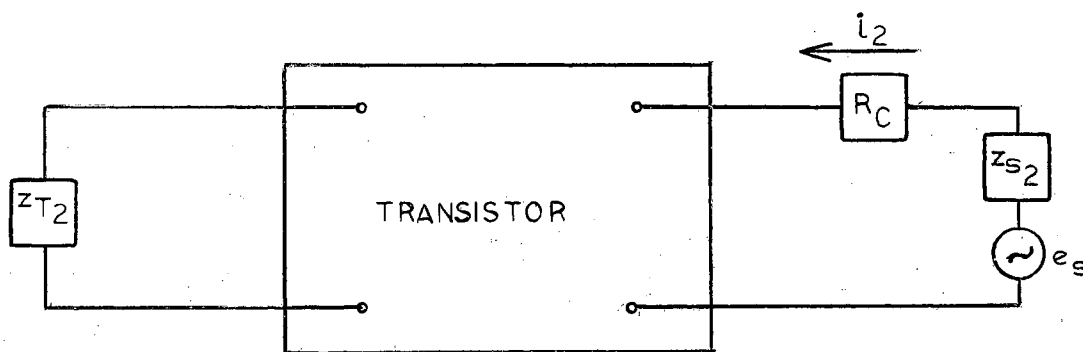


Figure I-4. h_{22} Measurement Circuit

The effect of the current sampling resistor in the circuit of Figure I-4 can be compensated for by simply adding this resistance to the source impedance and hence accounting for it in S.E.F.₂₂.

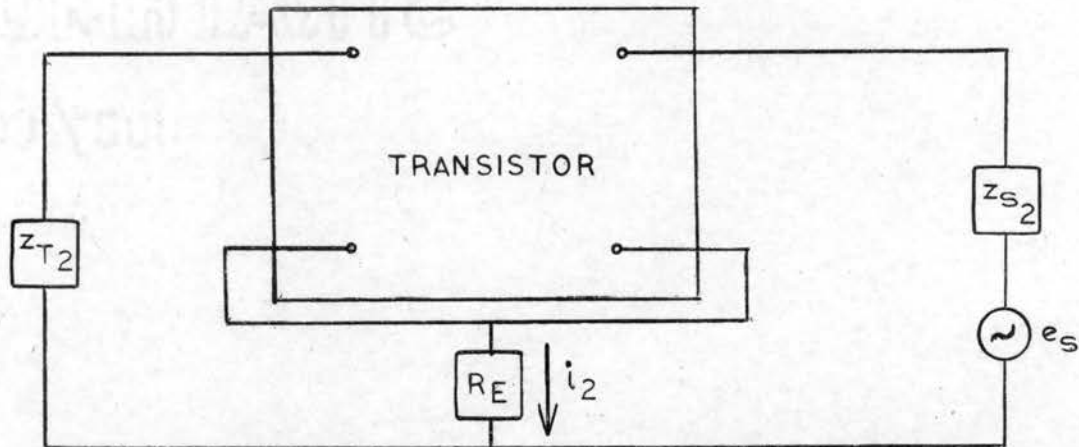


Figure I-5. h_{22} Measurement Circuit

The effect of the current sampling resistor, R_E , in the circuit of Figure I-5 on the measurement of h_{22} is slightly more complicated than that in Figure I-4. The error induced by the resistor in this measuring circuit can be found by replacing the fourpole of Figure I-5 with its h parameter equivalent circuit and writing loop equations which can be solved for i_2 in terms of v_2 . The result of this calculation, $\frac{i_2}{v_2}$, when compared with h_{22} will give an indication of how R_E affected the measurement of h_{22} . This analysis is done for the circuit in Figure I-6. To simplify this analysis the Thévenin equivalent of $h_{21} i_1$ in parallel with h_{22} is used. Also z_{s2} is neglected and presumed to be accounted for in the S.E.F.₂₂. Writing loop equations for the circuit in Figure I-6 we obtain

$$\begin{aligned}
 h_{12} v_2 &= -i_1(z_{T2} + h_{11} + R_E) - i_2 R_E \\
 v_2 &= i_1 \left(R_E - \frac{h_{21}}{h_{22}} \right) + i_2 \left(1/h_{22} + R_E \right)
 \end{aligned}
 \tag{I-29}$$

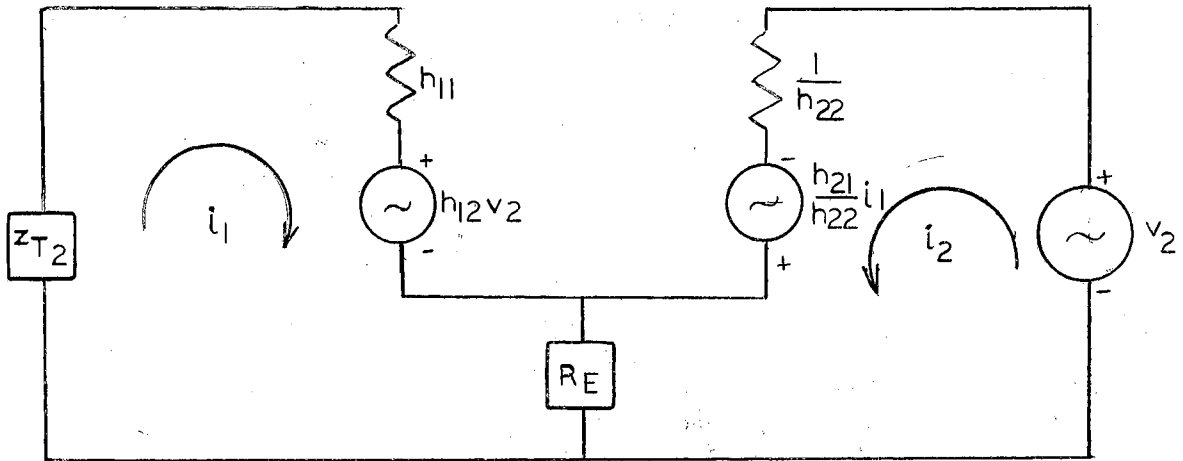


Figure I-6. h_{22} Measurement Circuit

Solving Equations (I-29) for i_2 we find

$$i_2 = \frac{v_2 \left[- (z_{T_2} + h_{11} + R_E) - h_{12} R_E + \frac{h_{12} h_{21}}{h_{22}} \right]}{\left[- (z_{T_2} + h_{11} + R_E) (1/h_{22} + R_E) + R_E^2 - \frac{R_E h_{21}}{h_{22}} \right]} \quad (\text{I-30})$$

In general, the order of magnitude of the terms in Equation (I-30) permit a close approximation to i_2 as follows:

$$i_2 \approx \frac{\left[v_2 \left[- (z_{T_2} + h_{11} + R_E) + \frac{h_{12} h_{21}}{h_{22}} \right] \right]}{\left[- (z_{T_2} + h_{11} + R_E) 1/h_{22} - \frac{R_E h_{21}}{h_{22}} \right]} \quad (\text{I-31})$$

Rewriting Equation (I-31) we find

$$h_{22} \approx \frac{i_2}{v_2} \left[\frac{z_{T_2} + h_{11} + R_E (1 + h_{21})}{z_{T_2} + h_{11} + R_E - \frac{h_{12} h_{21}}{h_{22}}} \right] \quad (\text{I-32})$$

Hence the T.E.F.₂₂ which compensates for the effect of R_E is

$$\frac{z_{T_2} + h_{11} + R_E - \frac{h_{12} h_{21}}{h_{22}}}{z_{T_2} + h_{11} + R_E (1 + h_{21})}$$

An approximation to this T.E.F.₂₂ can be found from the T.E.F.₂₂ derived previously and given in Table I-2 by dividing z_{T_2} by $(1 + h_{21})R_E + h_{11}$ instead of h_{11} . That is

$$\text{T.E.F.}_{22(R_E)} = 1 - \left(\frac{h_{12} h_{21}}{h_{22} h_{11}} \right) \left(\frac{1}{1 + \frac{z_{T_2}}{h_{11} + (1 + h_{21}) R_E}} \right)$$

The physical reason for this change might be considered to be the change in input impedance with R_E . With R_E equal to zero, the input impedance of the device is approximately h_{11} . We previously required that $z_T \gg h_{11}$ for the open circuit input condition to be satisfied. With R_E in the circuit, however, voltage feedback causes the input impedance to increase by an amount equal to $(1 + h_{21})R_E$ and hence now we require that $z_T \gg (1 + h_{21})R_E + h_{11}$. This factor must be considered when the common emitter h_{22} is being measured as it is quite possible that the open circuit termination condition is not as sufficient as it might ordinarily appear.

CHAPTER II

COMMON EMITTER h PARAMETER MEASUREMENTS

Common emitter h parameter measurement circuits, similar to those used by Texas Instruments, Inc., were built to ascertain the validity of the error factors proposed in Chapter I. Since a well established standard for h parameter measurements does not exist, the objective of this experiment was to investigate whether the error factors yielded consistent results. The same transistor was tested with various terminating and calibrating impedances, and the corrected results were compared.

The circuit shown in Figure II-1 was used to measure h_{11} and h_{21} at 1,000 c.p.s.

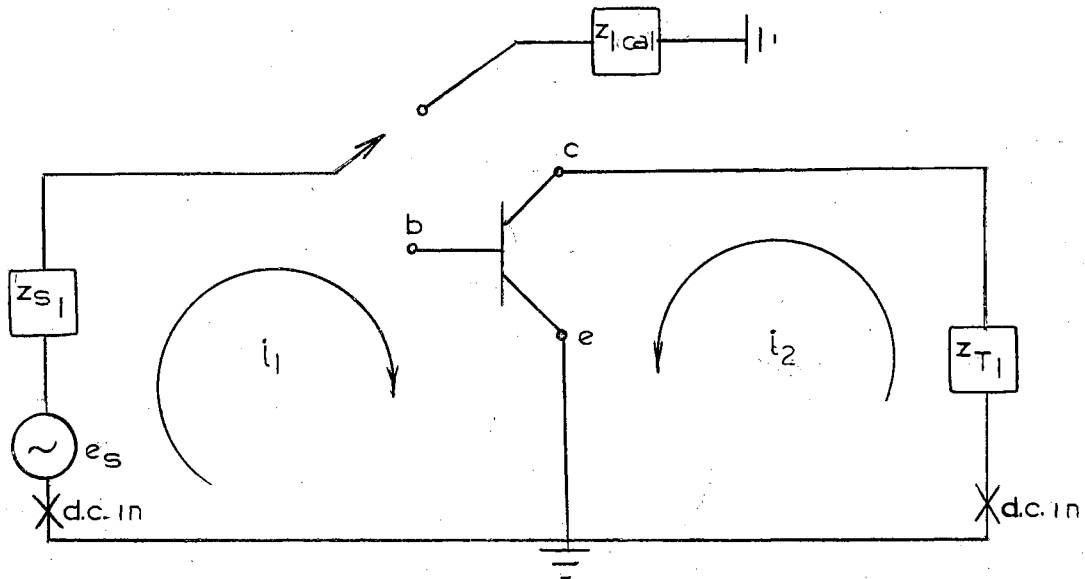


Figure II-1. h_{11} and h_{21} Measurement Circuit

The finite termination, z_{T_1} , which was necessary for the measurement of i_2 , induced errors in the measurement of h_{11} and h_{21} ; and, as stated previously, it was the purpose of this experiment to see whether these errors could be compensated for by using termination error factors. Likewise the current test signal, i_1 , deviates from a measured calibrate current, $i_{1 \text{ cal}}$, since $z_{1 \text{ cal}}$ is not generally equal to the input impedance of the device under test. It was desired to correct for this error by using a source error factor.

Calibration of this circuit was accomplished by adjusting the magnitude of the driving voltage until a 1 millivolt drop across $z_{1 \text{ cal}}$ implied a test current, $i_{1 \text{ cal}}$, of 1 amp. Since

$$h_{11} \approx \frac{v_1}{i_{1 \text{ cal}}} \approx v_1 (\text{volts}) \times 10^{-6} \approx v_1 (\text{mv}) \times 10^{-3} ,$$

the magnitude of the base to ground a.c. voltage in millivolts times 1,000 yields the measured parameter h_{11} . Since

$$h_{21} \approx \frac{i_2}{i_{1 \text{ cal}}} \approx \frac{v_{T_1}}{z_T i_{1 \text{ cal}}} \approx \frac{v_{T_1}}{z_{T_1}} (\text{mv}) \times 10^3 ,$$

the magnitude of the a.c. voltage in millivolts across z_{T_1} times $\frac{1,000}{z_{T_1}}$ yields the measured parameter h_{21} .

Several transistors were tested under various termination and source impedance conditions, and the results of this test for a typical transistor are tabulated. The device tested was a Texas Instrument 2N338 silicon transistor. In order to compute T.E.F.₁₁ and T.E.F.₂₁ the results of the measurements of h_{12} and h_{22} are needed. Hence in the calculations the value used for h_{22} was $4.5 \times 10^{-5} \text{ } \text{O}$ and the value used for h_{12} was 0.7×10^{-3} .

The circuit shown in Figure II-2 was used to measure h_{12} and h_{22} at 1,000 c.p.s.

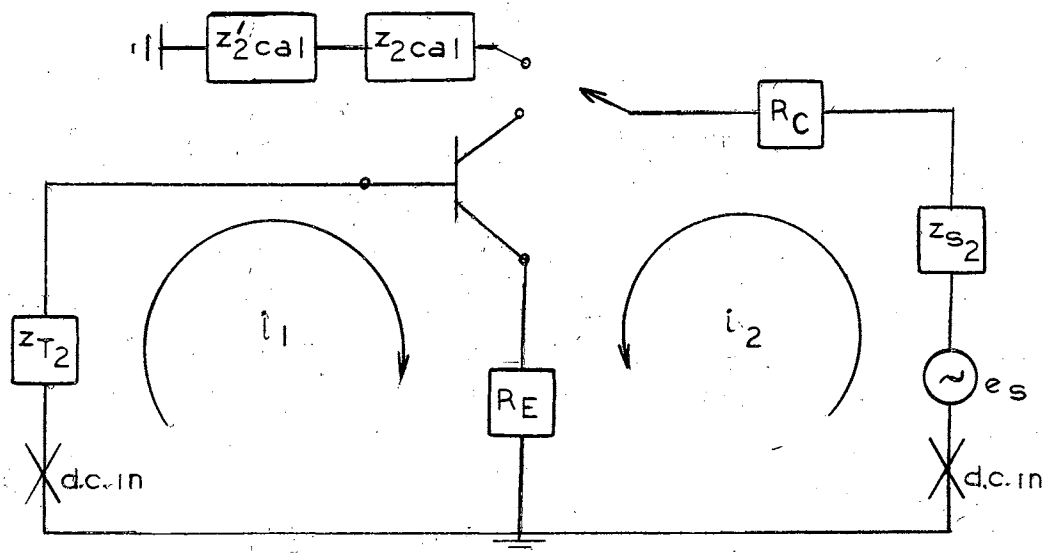


Figure II-2. h_{12} and h_{22} Measurement Circuit

Here parameter measurement errors resulted for several reasons. Since it was necessary that $i_1 \rightarrow 0$, a termination impedance, z_{T2} , which had infinite a.c. impedance was required. In addition to having infinite a.c. impedance, z_{T2} must be part of the d.c. biasing scheme; hence we necessarily have a finite termination impedance, z_{T2} . The error which results from a finite z_{T2} is magnified if we choose to use a current sampling resistor R_E , and as a result we must use a modified termination error factor when this is the case. Lastly the voltage test signal deviates from a measured calibrate signal since we do not have a perfect voltage source, and $z_{2\text{ cal}}$ is not necessarily equal to the output impedance of the device under test.

Calibration of the circuit shown in Figure II-2 was accomplished by adjusting the magnitude of the driving voltage until a 1 millivolt drop across $z'_{2\text{ cal}}$ implied a test voltage of 1 volt. Since

$$h_{22} \approx \frac{i_2}{v_2 \text{ cal}} \approx \frac{V_c}{R_c v_2 \text{ cal}} \approx \frac{V_E}{R_E v_2 \text{ cal}}$$

$$\approx v_c \text{ (millivolts)} \times \frac{10^{-3}}{R_c} \approx V_E \text{ (millivolts)} \times \frac{10^{-3}}{R_E},$$

the magnitude of the a.c. voltage in millivolts across R_c times $\frac{10^{-3}}{R_c}$ or the magnitude of the a.c. voltage in millivolts across R_E times $\frac{10^{-3}}{R_E}$ yields the measured parameter h_{22} . Since

$$h_{12} \approx \frac{v_1}{v_2 \text{ cal}} \approx v_1 \text{ (millivolts)} \times 10^{-3},$$

the magnitude of the base to ground a.c. voltage in millivolts times 10^{-3} yields the measured parameter h_{12} .

The results of h_{12} and h_{22} measurements for various terminations and methods of current sampling on a single device are tabulated. In order to compute T.E.F.₁₂ and T.E.F.₂₂ the results of the measurements of h_{11} and h_{21} are needed. In these calculations the value used for h_{11} was 2,600 ohms, and the value used for h_{21} was 130. $z'_{T_2} = z_{T_2} + z_c$ was used in the S.E.F. calculations.

A comparison of calculated parameters for the various termination and source impedances shows that adequate error compensation can be made if certain restrictions are placed on the values of the termination impedances relative to the transistor's input and output impedances.

In the measurement of h_{11} and h_{21} the range of termination impedance used was 100 ohms to 10,000 ohms, and the corresponding variation of the measured parameters was approximately 20 percent. The corrected parameters for the various terminations were within

+3 percent of a mean value. Note that in the extreme case the device output impedance, $1/h_{22}$, which was approximately 20,000 ohms, was only twice the value of the termination impedance.

In the measurement of h_{12} and h_{22} the value of termination impedance required was more stringent than that required for the h_{11} and h_{21} measurement. The measured parameters have a more pronounced effect on the correction factors in this case, and $z_{T2} \approx 5 [h_{11} + (h_{21} + 1) RE]$ results in measured parameters which when corrected will be within +5 percent of a mean value. In all cases the accuracy with which the voltmeter can be read is at most two significant figures, and this accounts in part for the variation in parameter values with termination.

TABLE II-1

RESULTS OF h_{11} AND h_{21} MEASUREMENTS UNDER
VARIOUS TERMINATION CONDITIONS

Measurement Condition	S.E.F. ₁₁	T.E.F. ₁₁	Measured h_{11}	Corrected h_{11}
	S.E.F. ₂₁	T.E.F. ₂₁	Measured h_{21}	Corrected h_{21}
$z_{T1} = 100\Omega$	0.93	1.0	2,600 Ω	2,800 Ω
$z_{S1} = 20\text{ K}\Omega$	0.93	1.0	132	142
$z_{T1} = 1,000\Omega$	0.94	0.97	2,500 Ω	2,725 Ω
$z_{S1} = 20\text{ K}\Omega$	0.94	0.96	130	144
$z_{T1} = 10,000\Omega$	0.95	0.83	2,100 Ω	2,650 Ω
$z_{S1} = 20\text{ K}\Omega$	0.95	0.78	105	141
$z_{T1} = 100\Omega$	0.95	1.0	2,500 Ω	2,625 Ω
$z_{S1} = 27\text{ K}\Omega$	0.95	1.0	132	138
$z_{T1} = 1,000\Omega$	0.96	0.97	2,400 Ω	2,600 Ω
$z_{S1} = 27\text{ K}\Omega$	0.96	0.96	125	136
$z_{T1} = 10,000\Omega$	0.96	0.83	2,200 Ω	2,750 Ω
$z_{S1} = 27\text{ K}\Omega$	0.96	0.78	102	136

TABLE II-2

RESULTS OF h_{12} AND h_{22} MEASUREMENTS UNDER
VARIOUS TERMINATION CONDITIONS

Measurement Condition	S.E.F. ₁₂	T.E.F. ₁₂	Measured h_{12}	Corrected h_{12}
	S.E.F. ₂₂	T.E.F. ₂₂	Measured h_{22}	Corrected h_{22}
$z_{T2} = 27 \text{ K}\Omega$ $z^1_{s2} = 50 \Omega$ $R_c = 0$ $R_E = 100 \Omega$	1.00	0.91*	0.7×10^{-3}	0.78×10^{-3}
	1.00	0.57	$2.9 \times 10^{-5} \text{ V}$	$5. \times 10^{-5} \text{ V}$
$z_{T2} = 27 \text{ K}\Omega$ $z^1_{s2} = 50 \Omega$ $R_c = 0$ $R_E = 1,000 \Omega$	1.00	0.91	0.7×10^{-3}	0.81×10^{-3}
	1.00	**	$9.4 \times 10^{-6} \text{ V}$	**
$z_{T2} = 27 \text{ K}\Omega$ $z^1_{s2} = 150 \Omega$ $R_c = 100 \Omega$ $R_E = 0$	1.00	0.91	0.7×10^{-3}	0.78×10^{-3}
	1.00	0.93	$4.5 \times 10^{-5} \text{ V}$	$4.75 \times 10^{-5} \text{ V}$
$z_{T2} = 27 \text{ K}\Omega$ $z^1_{s2} = 1,050 \Omega$ $R_c = 1,000 \Omega$ $R_E = 0$	0.95	0.91	0.7×10^{-3}	0.78×10^{-3}
	0.95	0.93	$4.5 \times 10^{-5} \text{ V}$	$5.1 \times 10^{-5} \text{ V}$
$z_{T2} = 50 \text{ K}\Omega$ $z^1_{s2} = 1,050 \Omega$ $R_c = 1,000 \Omega$ $R_E = 1,000 \Omega$	0.95	0.95	0.7×10^{-3}	0.78×10^{-3}
	0.95	0.65	$1.6 \times 10^{-5} \text{ V}$	$2.8 \times 10^{-5} \text{ V}$

TABLE II-2 (CONTINUED)

$z_{T_2} = 50 \text{ K}\Omega$ $z_{s_2}^1 = 1,050\Omega$ $R_C = 1,000\Omega$ $R_E = 0$	0.95	0.95	$.7 \times 10^{-3}$	0.78×10^{-3}
	0.95	0.93	$4.6 \times 10^{-5} \text{ V}$	$5.2 \times 10^{-5} \text{ V}$
$z_{T_2} = 5 \text{ K}\Omega$ $z_{s_2}^1 = 1,050\Omega$ $R_C = 1,000\Omega$ $R_E = 1,000\Omega$	0.95	0.65	0.4×10^{-3}	0.65×10^{-3}
	0.95	**	$0.19 \times 10^{-6} \text{ V}$	**
$z_{T_2} = 5 \text{ K}\Omega$ $z_{s_2}^1 = 1,050\Omega$ $R_C = 1,000\Omega$ $R_E = 0$	0.95	0.65	0.4×10^{-3}	0.65×10^{-3}
	0.95	**	$0.38 \times 10^{-6} \text{ V}$	**

* R_E is used in measurement of h_{22} only.

** Negative error factors are not defined.

CHAPTER III

COMMON EMITTER h PARAMETER MEASUREMENT CIRCUITS

It was desired to design a circuit which could be used to measure low frequency common emitter h parameters. One of the major characteristics of the final design is that the error factors be essentially unity, and hence close approximations to the parameters can be read directly on a voltmeter after circuit calibration. A combination of termination and source impedances were selected which would minimize the effect of finite or non-zero impedance terminations on the measured parameters, and at the same time permit the measurements to be made at a relatively high voltage level to minimize the effect of noise voltage on the measurements.

h_{11} and h_{21} Measurement Circuit

The circuit shown in Figure III-1 was designed to measure h_{11} and h_{21} for the common emitter configuration. The measuring frequency is 1,000 c.p.s.

Calibration (h_{11})

Two D.P.D.T. switches, s_3 and s_4 , are used to adjust base bias current polarity and collector voltage polarity. Proper positions of s_3 and s_4 are determined by transistor type, i.e., pnp or npn. The bias

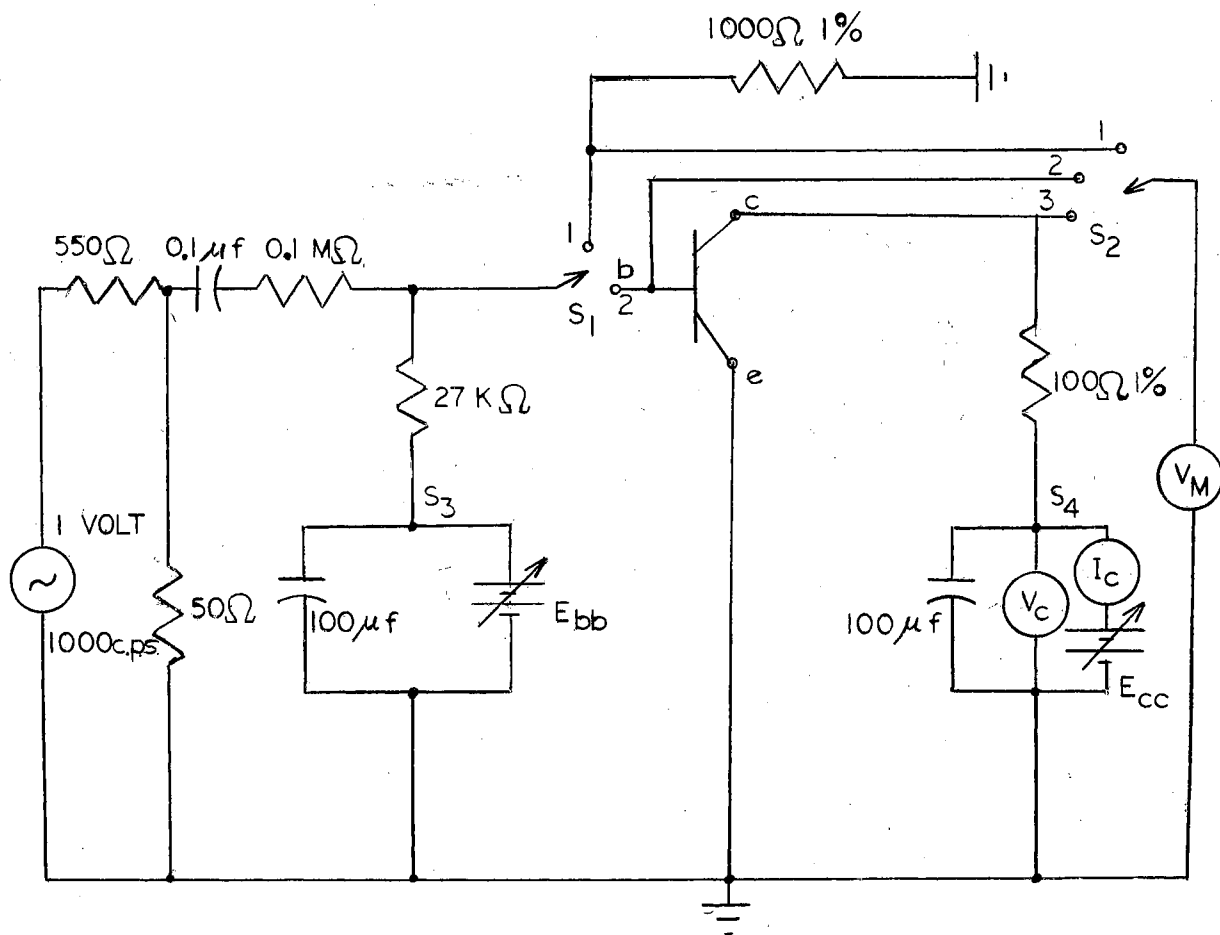


Figure III-1. h_{11} and h_{21} Measurement Circuit

power supplies are zeroed and s_3 and s_4 are set. Circuit calibration is accomplished with s_1 and s_2 in position 1. Note that s_3 must be in a position such that the base bias circuit is part of the calibration circuit. The a.c. supply voltage is adjusted to give a 1 millivolt deflection on the voltmeter, V_M , which implies a calibrate current of 1μ amp.

Measurement (h_{11})

With s_1 in position 2 and s_2 in position 3 the desired base bias current and collector voltage are obtained by adjustment of E_{bb} and E_{cc} .

An approximate value of h_{11} is read directly on V_M which is calibrated to read 1,000/millivolt.

Calibration (h_{21})

No change from calibration for h_{11} measurement.

Measurement (h_{21})

With s_1 and s_2 in position 2 bias adjustments are made. An approximate value of h_{21} is read directly on V_M which is calibrated to read 10/millivolt.

h_{12} and h_{22} Measurement Circuit

The circuit shown in Figure III-3 was designed to measure h_{12} and h_{22} for the common emitter configuration. Again the measuring frequency is 1,000 c.p.s.

It was found that the collector biasing scheme shown in Figure III-3 had certain advantages over a shunt-feed system shown in Figure III-2. The inductance and Q requirements of the coil shown in Figure III-2 were particularly stringent, especially when the allowable d.c. collector current level was greater than 50 milliamps.

The center-tapped transformer feed system shown in Figure III-3 allowed a means of balancing the d.c. saturation of the transformer core. Here a variable dummy load can be adjusted so that mmf of the d.c. collector current and the mmf of the dummy load current cancel.

Calibration (h_{12})

Proper bias polarities are determined and s_3 and s_4 are set accordingly. Circuit calibration is accomplished with s_1 and s_2 in

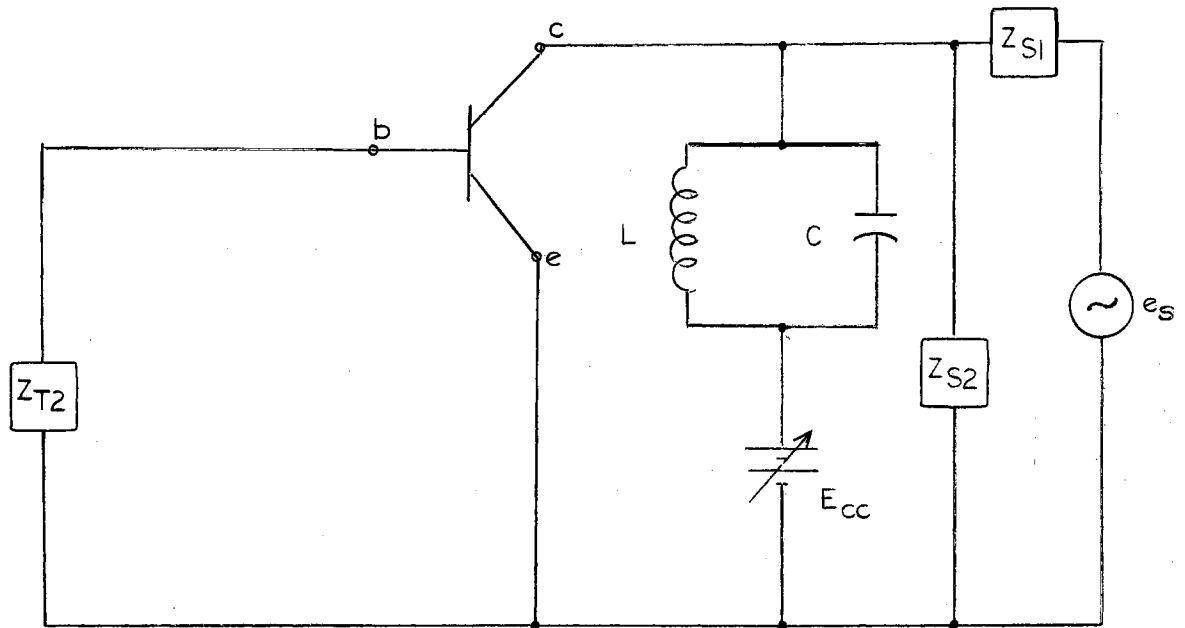
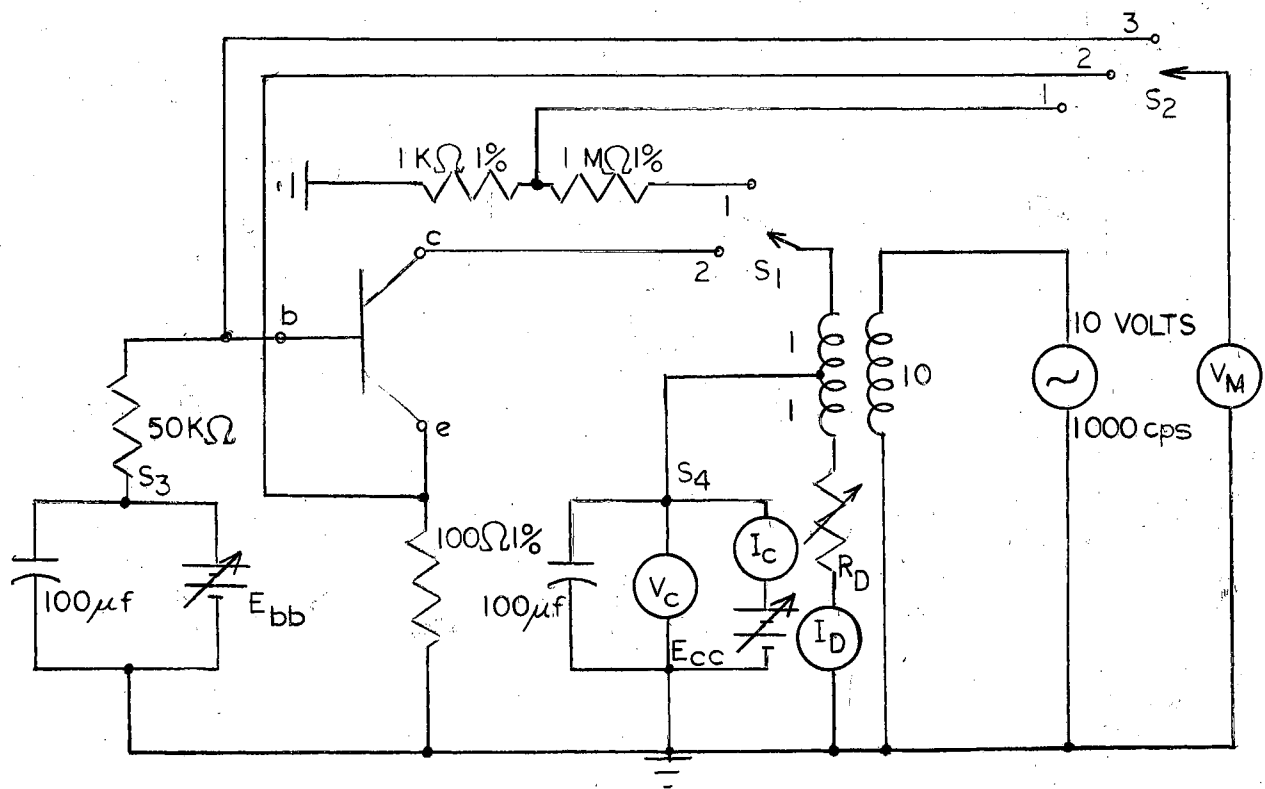


Figure III-2. Collector Biasing Scheme

Figure III-3. h_{12} and h_{22} Measurement Circuit

position 1. The a.c. supply voltage is adjusted to give a 1 millivolt deflection on V_M which implies a calibrate voltage of 1 volt.

Measurement (h_{12})

With s_1 in position 2 and s_2 in position 3 proper bias adjustments are made. R_D is adjusted to give a dummy load current equal to the d.c. collector current. An approximate value of h_{12} is read on V_M which is calibrated to read 10^{-3} /millivolt.

Calibration (h_{22})

No change from calibration for h_{12} measurement.

Measurement (h_{22})

With s_1 and s_2 in position 2 proper bias adjustments are made. R_D is adjusted to give a dummy load current equal to the d.c. collector current. An approximate value of h_{22} is read directly on V_M which is calibrated to read 10^{-5} \mathcal{U} /millivolt.

CHAPTER IV

FREQUENCY DEPENDENCE OF h_{21}

Introduction

It is important to ascertain the frequency range for which the transistor may be represented by real h parameters. There is some difficulty involved in determining the discrete frequency limitations, and obviously the selection of limits is a function of the accuracy required of the equivalent circuit. Fortunately the h parameters are essentially independent of frequency in this range. At higher frequencies it becomes necessary to use complex h parameters, which in general are valid only for the measurement frequency. The high frequency dependence of the h parameters is difficult to obtain, and for this reason it is customary to use equivalent T or π circuits at higher frequencies.

Several approximations of the frequency dependence of the transistor current gain, α i.e. h_{21} for the common base configuration, have been made. The following analysis closely parallels the work done by B. F. C. Cooper (5) which appeared in the article, "A Bridge for Measuring Audio Frequency Transistor Parameters." A first approximation to α is

$$\alpha = \frac{\alpha_0}{1 + jK (f/f_\alpha^0)} \quad (\text{IV-1})$$

which considers the finite transit time of minority carriers crossing the base region. α_0 is the low-frequency current-amplification factor, f_{α}^{co} is the frequency where $|\alpha|$ is $0.707 \alpha_0$, and K is a constant whose value depends upon the process giving rise to the cutoff. The theoretical value for K is 1.21 when cutoff is determined by the transit time of minority carriers crossing the base.

At low frequencies (IV-1) may be approximated by

$$\alpha = \alpha_0 (1 - jKf/f_{\alpha}^{co}), \quad 1 \gg K^2 f^2 / f_{\alpha}^{co^2} \quad (IV-2)$$

f_{α}^{co} might possibly be evaluated by measuring the phase lag, $\tan^{-1} Kf/f_{\alpha}^{co}$, at a known frequency. If the measuring frequency is too low to obtain sufficient accuracy, the phase lag of the common emitter current gain, which is considerably greater than the phase lag of the common base current gain, may be measured.

Since

$$a_{ce} \approx \frac{a}{1 - a} \quad (IV-3)$$

substituting Equation (IV-1) into Equation (IV-3) we obtain

$$a_{ce} \approx \frac{\frac{\alpha_0}{1 + jKf/f_{\alpha}^{co}}}{1 - \frac{\alpha_0}{1 + jKf/f_{\alpha}^{co}}} \quad (IV-4)$$

$$a_{ce} \approx \frac{\alpha_0}{(1 - \alpha_0 + jKf/f_{\alpha}^{co})} \quad (IV-5)$$

Hence if $(1 - \alpha_0) \ll Kf/f_{\alpha}^{co}$, Equation (IV-5) can be approximated by

$$a_{ce} \approx \frac{\alpha_0}{(1 - \alpha_0)^2} [(1 - \alpha_0) - jKf/f_{\alpha}^{co}]$$

$$\alpha_{ce} \approx \frac{\alpha_o}{(1 - \alpha_o)} [1 - jKf/f_{\alpha}^{co} (1 - \alpha_o)] \quad (IV-6)$$

The phase lag of α_{ce} , $\tan^{-1} Kf/f_{\alpha}^{co} (1 - \alpha_o)$, as seen from Equation (IV-6) is greater than the phase lag of α because of the factor, $\frac{1}{1 - \alpha_o}$.

A technique for measuring the complex parameter h_{21} is discussed in the next section, and this complex parameter is used in conjunction with Equation (IV-6) to compute f_{α}^{co} .

A Bridge for Measuring h_{21}

Standard procedure in a.c. bridge measurements involves dealing with in-phase and quadrature components of terminal voltages and currents, and the result of this is that the parameters being measured will be complex valued. A modification of the bridge circuit which was designed by Mr. B. F. C. Cooper (6) was used to measure the complex ratio, h_{21} , for the common emitter configuration. The circuit which was designed by Mr. Cooper is shown in Figure IV-1, and the modification of this circuit follows.

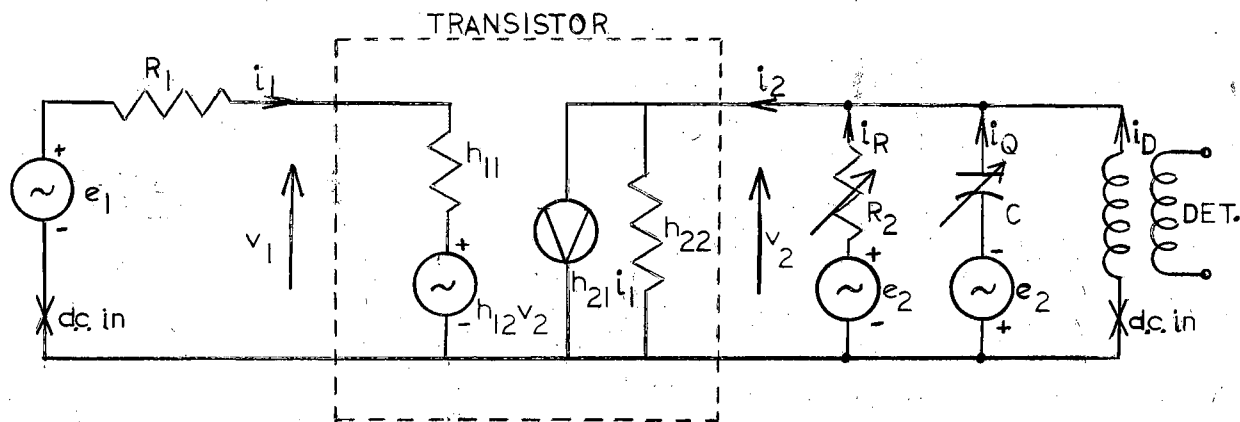


Figure IV-1. $R_e h_{21} + j I_m h_{21}$ Measurement Circuit

$$e_1 = k_1 e_o$$

$$e_2 = k_2 e_o$$
(IV-7)

The voltages e_1 and e_2 are exactly in phase. The k 's represent a variable magnitude of calibrated attenuator. The measurement frequency is 1,000 c.p.s. $i_D = 0$ implies

$$i_2 = i_R + i_Q$$
(IV-8)

$v_2 = 0$ at the same time implies

$$i_2 = h_{21} i_1 = h_{21} \frac{e_1}{R_1}$$
(IV-9)

Since

$$i_R = \frac{e_2}{R_2}$$
(IV-10)

$$i_Q = j\omega C e_2$$

Equations (IV-7), (IV-8), (IV-9), and (IV-10) may be combined to give the following result.

$$h_{21} = \frac{R_1 k_2}{R_2 k_1} (1 - j\omega C R_2)$$
(IV-11)

Equating the phase lag of α_{ce} from Equation (IV-6) with the phase lag of h_{21} (which is equal to α_{ce}) in Equation (IV-11) gives

$$f_{\alpha}^{co} = \frac{K}{(1 - \alpha_o)^2 C R_2}$$
(IV-12)

The circuit which was used to measure the complex current-amplification

factor is shown in Figure IV-2.

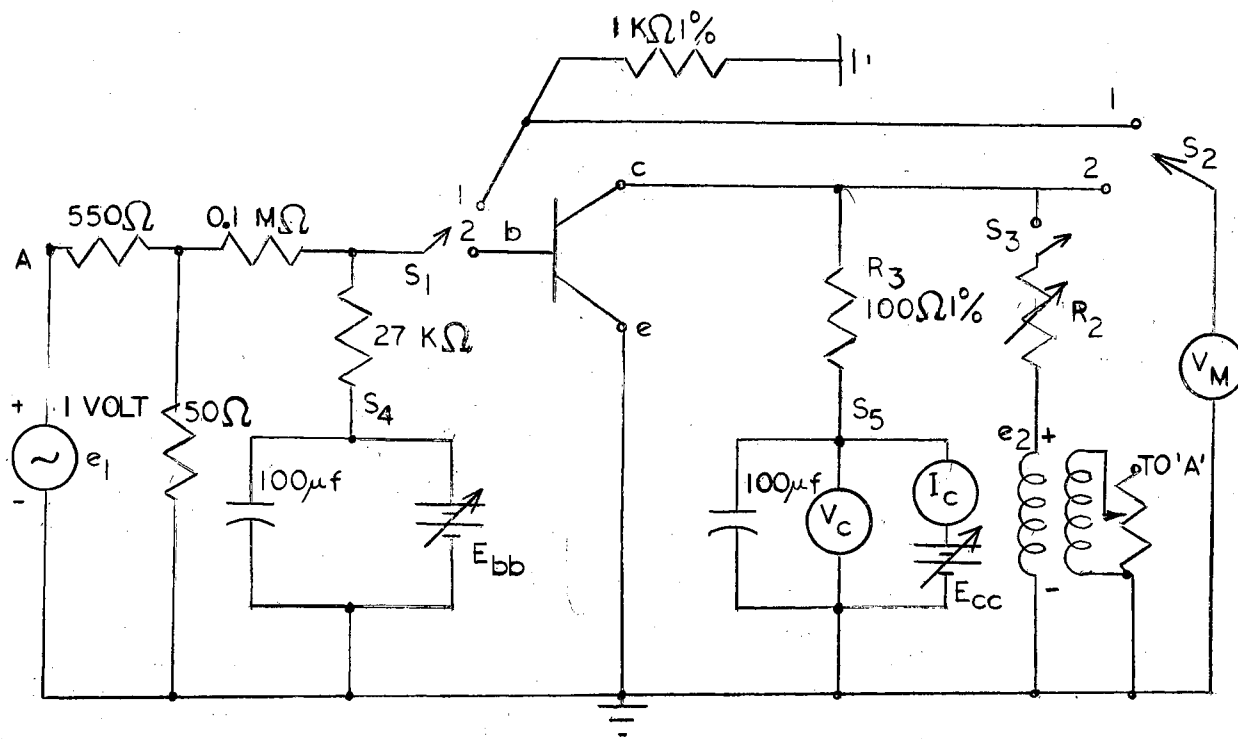


Figure IV-2. $R_e h_{21} + j I_m h_{21}$ Measurement Circuit

It is assumed that h_{11} has a negligible effect on the phase relationship between e_1 and i_1 , that is $R_1 \gg h_{11}$. The h parameter equivalent circuit with the a.c. measuring circuit corresponding to Figure IV-2 is shown in Figure IV-3.

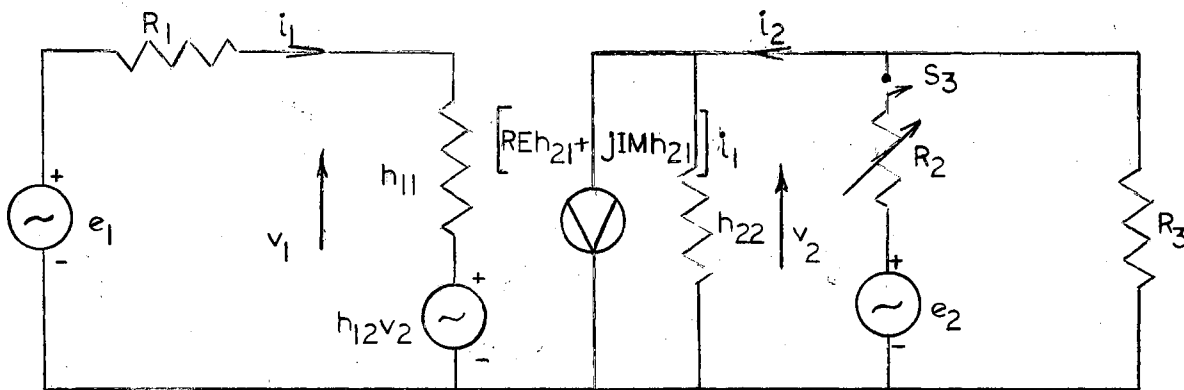


Figure IV-3. $R_e h_{21} + j I_m h_{21}$ Measurement Circuit

The current generator and parallel conductance are replaced by their Thévenin equivalents and Figure IV-3 is redrawn below.

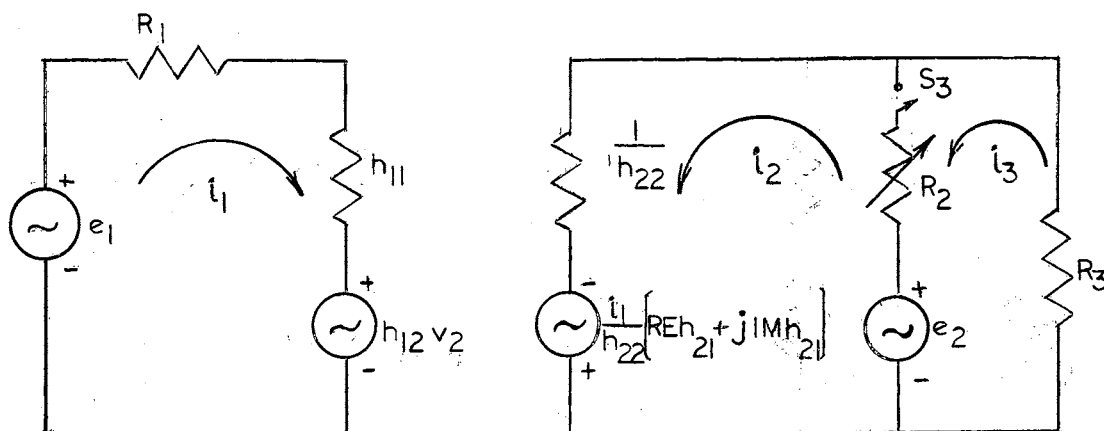


Figure IV-4. $R_e h_{21} + j I_m h_{21}$ Measurement Circuit

With s_3 open

$$i_3 = \frac{-\frac{1}{h_{22}} [R_e (h_{21}) + j I_m (h_{21})] i_1}{\frac{1}{h_{22}} + R_3} \quad (IV-13)$$

If $R_3 \ll \frac{1}{h_{22}}$,

$$i_3 \approx |h_{21}| i_1 \quad (IV-14)$$

and a voltage proportional to i_3 , i.e., $i_3 R_3$ permits evaluation of $|h_{21}|$.

Next the possibility of measuring the imaginary component of the current gain, $I_m h_{21}$, is investigated, and to do this the conditions which must be met in order to eliminate the real part of the current, i_3 , are of interest. With s_3 closed the loop equations for the output circuit are written. Superposition is used to simplify the analysis and the in-phase voltages $\frac{i_1 R_e}{h_{22}} (h_{21})$ and e_2 are considered.

$$\frac{i_1}{h_{22}} \operatorname{Re}(h_{21}) + e_2 = i_2(1/h_{22} + R_2) - i_3 R_2 \quad (\text{IV-15})$$

$$-e_2 = -i_2 R_2 + i_3 (R_2 + R_3)$$

From Equations (IV-15)

$$i_3 = \frac{-(1/h_{22} + R_2) e_2 + R_2 [i_1/h_{22} \operatorname{Re}(h_{21}) + e_2]}{(1/h_{22} + R_2) (R_2 + R_3) - R_2} \quad (\text{IV-16})$$

From Equation (IV-16) we find that if $\frac{e_2}{R_2} = i_1 \operatorname{Re}(h_{21})$, the real part of the current i_3 is zero.

If the proper adjustment of e_2 and R_2 can be obtained with $R_2 \approx 10 R_3$ the current i_3 is $i_1 [\operatorname{Im} h_{21}]$. Hence the imaginary part of h_{21} , $\operatorname{Im} h_{21}$, is measurable. R_2 should be approximately $10 R_3$ so that R_2 will have a negligible effect on the quadrature component of i_3 .

Circuit Operation

Calibration ($R_e h_{21} + j I_m h_{21}$)

The bias power supplies are adjusted as in the measurement of h_{21} . Circuit calibration is accomplished with s_1 and s_2 in position 1, and s_3 open. The a.c. supply voltage is adjusted to give a 1.0 millivolt deflection on the voltmeter, V_M , which implies a calibrate current of 1μ amp.

Measurement ($R_e h_{21} + j I_m h_{21}$)

With s_1 and s_2 in position 2 and s_3 open, proper bias adjustments are made. An approximate value of h_{21} is read on V_M which is calibrated to read 10/millivolt. s_3 is then turned on, and the values of e_2 and R_2 are adjusted until the V_M reading is minimized. This

minimum reading is the quadrature component of h_{21} , $I_m(h_{21})$. Thus h_{21} can be written in terms of in-phase and quadrature components, i.e., $R_e(h_{21}) + j I_m(h_{21})$, and f^{CO} can be predicted by

$$\sin^{-1} \frac{I_m(h_{21})}{h_{21}} = \tan^{-1} \frac{Kf}{f_{\alpha}^{CO} (1 - \alpha_o)} \quad (IV-17)$$

The transformer which was used in the circuit of Figure IV-2 was a UTC audio unit Type No. A-20. Its frequency response was flat from 20 c.p.s. to 30 K c.p.s. The voltmeter which was used in the preliminary measurements was a Hewlett Packard Model 302A Wave Analyzer. Very little difference in voltage readings was noticed between this highly selective voltmeter and a Hewlett Packard Model 400 D VTVM.

The primary objective of this part of the study was to make low frequency measurement of the complex current gain, and use Equation (IV-13) to determine f_{α}^{CO} and the common emitter h_{21} cutoff frequency.

Measurements were made on approximately 20 transistors. The complex ratio h_{21} was measured at several frequencies in the range 100 c.p.s. to 5,000 c.p.s. for each device. f_{α}^{CO} was calculated for the device using Equation IV-17, and this number was divided by h_{21} to give the common emitter cutoff frequency. The calculated common emitter cutoff frequency, $f_{\alpha E}^{CO}$, was compared to the measured $f_{\alpha E}^{CO}$, and in all cases the calculated results were within ten percent of the measured values in the frequency range of from 5,000 to 20,000 c.p.s.

At a low frequency relative to the device cutoff frequency, $f_{low} < (\frac{1}{100}) (f_{\alpha E}^{CO})$, the $R_2 - e_2$ balance adjustment is very critical and practically impossible to obtain. At a fairly high frequency relative to the device cutoff frequency, $f_{high} > 1/5 f_{\alpha E}^{CO}$, the

parameter h_{22} becomes complex and the original analysis is invalid. In general measurements taken at frequencies within these limits yielded consistent results for the $f_{\alpha E}^{\text{co}}$.

CHAPTER V

CONCLUSION

The primary objective of this study was to investigate existing methods of h parameter measurement with the intent of simplifying existing techniques where possible. As stated previously the advantage of using the hybrid equivalent circuit is that since the transistor is inherently a low input impedance and high output impedance device the terminations required when making the h parameter measurements are not difficult to obtain. It is generally desired that the termination impedances differ by at least two orders of magnitude from the transistor input or output impedances. This means that $z_{T_1} \simeq \frac{1}{100} \left[\frac{1}{h_{22}} \right]$ and $z_{T_2} \simeq 100 h_{11}$. If termination errors are compensated for, it is conceivable that $z_{T_1} \simeq \frac{1}{5} \left[\frac{1}{h_{22}} \right]$ and $z_{T_2} \simeq 5 h_{11}$ will yield results which, when corrected, are within five percent of the actual parameter values. The major advantages of this are that measurements of h_{21} and h_{22} can be made at a higher signal level, and the effects of noise on the results can be reduced. Also resistive termination impedances can be used, and noise problems introduced by the addition of inductors and tuned circuits are eliminated beforehand. Needless to say, cost is a factor as can be seen by the comparison of prices for high Q, high inductance coils with prices of resistors.

Since all a.c. voltages are measured with respect to the same

reference, it is quite convenient to use the standard CRO technique for determining whether the measured h parameters are complex. This could be done by applying a voltage proportional to the input signal to one pair of deflection plates, and a voltage which corresponds to the parameter being measured to the second pair of deflection plates. The resulting lissajous pattern will give some indication as to the phase shift between these voltages, and hence an indication of whether or not the parameter is complex valued.

In instances where it is necessary to measure the complex ratio h_{21} more accurately, the circuit shown in Figure IV-3 works satisfactorily at frequencies lower than 5,000 c.p.s. This circuit lends itself to the prediction of a transistor's h_{21} cutoff frequency and is particularly useful for common emitter cutoff frequencies of less than 20 K c.p.s. This includes transistors whose alpha cutoff frequency is in the 1-2 megacycle range. It would be interesting to investigate whether a technique similar to this would be useful for measurement of alpha cutoff in the 2-50 magacycle range. It is conceivable that a common emitter measuring frequency of 20 K c.p.s. would be possible.

The measuring circuits shown in Figures III-1 and III-3 can be readily adapted for use in sweep measurements. This possibility would require further investigation, but it appears that the h parameters could be measured at a constant frequency over a range of the transistor's $V_c - I_c$ characteristic by using either collector current or voltage as a parameter and sweeping the other variable over the range of interest. This can be done with little change in actual measuring circuitry. The only additional components required would be

an a.c. to d.c. voltage converter and a recorder. The error factors would permit one to predict measurement accuracy or possibly allow corrections of actual measurements.

BIBLIOGRAPHY

1. Gartner, W. W. Transistors: Principles, Design, and Applications. Princeton, New Jersey: D. Van Nostrand Company, Inc., 1960, pp. 213-224.
2. Follingstad, H. G. "An Analytical Study of z , y , and h Parameter Accuracies in Transistor Sweep Measurement." Institute of Radio Engineers Convention Record, Volume 2, 1954, p. 107.
3. Gartner, W. W. Transistors: Principles, Design, and Applications. Princeton, New Jersey: D. Van Nostrand Company, Inc., 1960, p. 217.
4. Follingstad, H. G. "An Analytical Study of z , y , and h Parameter Accuracies in Transistor Sweep Measurement." Institute of Radio Engineers Convention Record, Volume 2, 1954, p. 112.
5. Cooper, B.F.C. "Bridge for Measuring Audio-Frequency Transistor Parameters." Institute of Radio Engineers Proceedings, Volume 43, 1955, pp. 796-805.
6. Cooper, B.F.C. "Bridge for Measuring Audio-Frequency Transistor Parameters." Institute of Radio Engineers Proceedings, Volume 43, 1955, pp. 796-805.

VITA

Daniel M. Rukavina

Candidate for the Degree of

Master of Science

Thesis: TRANSISTOR h PARAMETER MEASUREMENT TECHNIQUES

Major Field: Electrical Engineering

Biographical:

Personal Data: Born in St. Cloud, Minnesota, February 12, 1937,
the son of Daniel G. and Clara M. Rukavina.

Education: Graduated from Greenway High School, Coleraine,
Minnesota, June, 1955; received the Bachelor of Science
Degree in Electrical Engineering from the Michigan College of
Mining and Technology, Houghton, Michigan, 1959; completed the
requirements for the Master of Science Degree in August, 1962.

Experience: Employed by Western Electric Company, Oklahoma City,
Oklahoma, as a product engineer from July, 1959, to September,
1960; taught in the School of Electrical Engineering, Oklahoma
State University, Stillwater, Oklahoma, from September, 1960,
to May, 1962.

Professional Organizations: N.S.P.E., O.S.P.E., and I.R.E.